Quantifying the effect of temporal resolution on time-varying networks

Bruno Ribeiro,[1] Nicola Perra,[2] and Andrea Baronchelli[2]

[1] *Computer Science Department, University of Massachusetts Amherst, USA*
[2] *Laboratory for the Modeling of Biological and Socio-technical Systems, Northeastern University, Boston MA 02115, USA*

Time-varying networks describe a wide array of systems whose constituents and interactions evolve over time. These networks are defined by an ordered stream of interactions between nodes. However, they are often represented as a sequence of static networks, resulting from aggregating all edges and nodes appearing at time intervals of size Δt. In this work we investigate the consequences of this procedure. In particular, we address the impact of an arbitrary Δt on the description of a dynamic process taking place upon a time-varying network. We focus on the elementary random walk, and put forth a mathematical framework that provides exact results in the context of synthetic activity-driven networks. Remarkably, the equations turn out to also describe accurately the behavior observed on real datasets. Overall, our analytical description of the bias introduced by time integrating techniques represents a step forward in the correct characterization of dynamical processes on time-varying graphs.

Time-varying networks are ubiquitous. Examples are found in the social, cognitive, technological and ecological domains as well as in many others [1]. The temporal nature of such systems has a deep influence on dynamical processes occurring on top of them [2–19]. Indeed, the spreading of sexual transmitted diseases, the diffusion of topics over social networks, and the propagation of ideas in scientific environments are affected by duration, sequence and concurrency of contacts [2, 4, 17–21]. In all these cases the timescale characterizing the evolution of the network is comparable with the timescale ruling the unfolding of the process, and they cannot be decoupled. However, empirical datasets are often reduced to a series of static networks by introducing a time-integrating window, Δt [1, 22–25]. Dynamical processes are then let evolve in the sequence of $T/\Delta t$ networks, where T is the total time span available. While this technique might be useful to gain different levels of insight into the dynamics of these processes, it might introduce strong biases in their characterization [1–3, 5, 6, 17, 18].

Beyond practical reasons, the interplay of timescales in the characterization of processes evolving on time-varying networks is a deep and general problem. The minimum time resolution achievable when measuring a network in the wild is likely to be finite, and a given Δt may be intrinsic to the description at hand. The latter is the case, for instance, of face-to-face interaction networks [26], for which the fine-grained temporal resolution of (e.g.) phone call networks is not available. Similarly, an intrinsic minimum time resolution might exist. Scientific reviews, for example, "aggregate" articles with the periodicity of their publication (e.g. weekly or monthly), which then becomes the timescale of the citation or co-authorship networks [27–29].

In this paper, we analyze the role played by an arbitrary Δt. We investigate in detail how the behavior of a dynamical process depends on the time aggregation window of the underlying time-varying graph. We focus our attention on the elementary random walk process (RW) and address explicitly the role of Δt in the behavior of the walker. Adopting the theoretical framework of activity-driven networks [17] (see Methods), we provide an analytical characterization of the RW asymptotic occupation probability as a function of Δt. The proposed mathematical framework yields a clear understanding of the effects introduced by time-aggregating techniques on the diffusion process, accurately describing the biases and distortions introduced by aggregation procedures. We explicitly connect our results to the well-known RW occupation probability on static networks and extensively prove our analytical results against numerical simulations on synthetic networks. We then extend our validation by considering a set of distinct real time-varying networks. Remarkably, also in this case the observed effects introduced by time aggregation are well described by our analytical results, which suggests their validity in a wide class of time-varying networks.

Results

We consider a random walker diffusing at discrete time steps Δt over a time-varying network characterized by N nodes[42]. Starting at node $V(t)$ at step t, the walker takes step $t+1$ at time $(t+1)\Delta t$ diffusing over a network $G_t(\Delta t)$, where $G_t(\Delta t)$ is the result of the union of all the edges generated in the interval $[t\Delta t, (t+1)\Delta t)$ (see Figure 1). We refer to Δt as the integrating time window of the network. In the limit $\Delta t \to 0$ the RW process and the network evolve on the same timescale, with the walker moving as soon as an edge appears. This limit has been studied analytically [18] in the framework of activity-driven networks [17], where each node is characterized by an activity rate describing the

average edge creation rate of a node in the system (see Methods). Here, we address the general case $\Delta t > 0$, which – as it will soon be clear – produce dramatically differently walker behaviors than the $\Delta t \to 0$ special case.

Activity-driven networks are a class of time-varying graphs characterized by two parameters (see Methods for further details): m, the number of edges that are simultaneously created by a node, and dF(a)[43], the fraction of nodes with activity rate a. The activity rate determines the probability per unit time of a node establishing (m, simultaneously) edges to other nodes in the system. The value of parameter m is dictated by the specific system under consideration. The case $m > 1$ is appropriate to describe one-to-many interactions, found for example in such systems as Twitter and blog networks [30, 31]. On the other hand, $m = 1$ describes two-party communications that are characteristic of phone-call and text-message networks [32, 33]. As we will see, the latter case is particularly relevant, and in the following sections we will refer to this type of systems as *time-varying dyadic networks*.

Analytic expression for arbitrary integrating windows.

Let us define $Q_{a|a'}(\Delta t)$ as the transition probability that a walker starting at a node with activity a' moves to a node with activity a at the next step. To find an expression for $Q_{a|a'}(\Delta t)$, note that at step $t+1$ the neighbors of $V(t)$ can be classified into two types:

1. *Passive destinations*, are neighbors of $V(t)$ connected by edges created due to the activity of $V(t)$ itself. The endpoints away from $V(t)$ are randomly sampled from the graph and thus their activity comes from the distribution $\mathrm{dF}(a)$. We define $m\,K_{\Delta t,A(t)}$ to be the number of such passive destinations.

2. *Active destinations*, are neighbors of $V(t)$ connected to $V(t)$ by edges created due to their own activity. The endpoint away from $V(t)$ is biased towards high-activity nodes. More precisely, the activity distribution of such node is $a\mathrm{dF}(a)/\langle a\rangle$, where $\langle a\rangle$ is the average activity rate. We define define $H_{\Delta t}$ as the number of such active destinations.

The word *destinations* highlights the fact that the walker moves from $V(t)$ to one of these $m\,K_{\Delta t,a'} + H_{\Delta t}$ nodes. For sufficiently large N, $H_{\Delta t}$ is Poisson distributed with average $m\langle a\rangle\Delta t$ and $K_{\Delta t,a'}$ is Poisson distributed with average $a'\Delta t$. If $V(t)$ has at least one edge, the walker chooses to follow the edge of a passive destination with probability $m\,K_{\Delta t,a'}/(m\,K_{\Delta t,a'} + H_{\Delta t})$. Conversely, the walker follows an edge towards an active destination with probability $H_{\Delta t}/(m\,K_{\Delta t,a'} + H_{\Delta t})$. Unconditioning the latter expression with respect to the values of $K_{\Delta t,a'}$ and $H_{\Delta t}$ we obtain for all values of a and a'

$$Q_{a|a'}(\Delta t) = \lim_{\epsilon\to 0}\sum_{k=0}^{\infty}\sum_{h=0}^{\infty}\left(\tfrac{m\,k}{m\,k+h+\epsilon}\mathrm{dF}(a) + \tfrac{h}{m\,k+h+\epsilon}\tfrac{a\,\mathrm{dF}(a)}{\langle a\rangle} + \tfrac{\epsilon}{m\,k+h+\epsilon}\delta(a-a')\right) \times \tfrac{(a'\Delta t)^k}{k!}\exp(-a'\Delta t) \times \tfrac{(m\langle a\rangle\Delta t)^h}{h!}\exp(-m\langle a\rangle\Delta t)\,, \tag{1}$$

where $\delta(a'-a)$ is the Dirac delta function which is one if $a' = a$ and zero otherwise, and $\epsilon \to 0$ is an auxiliary variable used to avoid treating special cases that lead to an undefined $0/0$ separately from the main equation. While we refer the reader to the Supplementary Information (SI) for the detailed derivation, each term in Eq. (1) has a simple interpretation. The first term inside the double sum is the probability that the walker moves to a passive destination that has activity a; the second term inside the double sum is the probability that the walker moves to an active destination that has activity a; the third term inside the double sum is the probability that the node has no edges after time Δt and thus the walker remains at $V(t)$, hence not changing activity; the first term at the second line gives the probability that $K_{\Delta t,a'} = k$ implying that km passive nodes are connected to $V(t)$; and finally the second term at the second line gives the probability that h active nodes are connected to $V(t)$.

The most interesting special case of Eq. (1) concerns time-varying dyadic networks ($m = 1$). In these networks Eq. (1) is greatly simplified (see SI):

$$Q_{a|a'}(\Delta t) = \frac{a'+a}{a'+\langle a\rangle}\mathrm{dF}(a)(1-\zeta_{a',\Delta t}) + \delta(a'-a)\zeta_{a',\Delta t}\,, \tag{2}$$

where $\zeta_{a',\Delta t} = e^{-(a'+\langle a\rangle)\Delta t}$ is the probability that no edge is created at a node with activity a' during interval Δt.

To find the RW stationary distribution we first note that the RW on the time-varying network is stationary and ergodic (see SI). Thus, the RW occupation probability ρ_a, defined as the probability of finding the walker in a given

node of activity a, exists and is unique [34]. The value of ρ_a is the fixed point solution of the following Chapman-Kolmorogov set of equations [35]

$$\rho_a = \frac{1}{N\mathrm{dF}(a)} \int_{a' \in \Omega} Q_{a|a'}(\Delta t)\rho_{a'}\mathrm{dF}(a')\,, \quad \forall a \in \Omega\,. \tag{3}$$

The solution to Eq. (3) can be easily obtained by numerical methods. However, for $\Delta t \to 0$ the equation admits a simple solution that reproduces the results in Perra et al.[18] (see SI). Next we see that in time-varying dyadic networks $\Delta t \ll 1$ and $\Delta t \gg 1$ are also special cases that admit closed-form solutions.

Static networks widely used in the research community are often the result of aggregating time-varying networks over large aggregating windows, $\Delta t \gg 1$ [1]. We connect our approach to static network results by contrasting the walker occupation probability ρ_a of a time-varying dyadic network (Eq. (3)) against the static network occupation probability ρ_k^{static} of a given static snapshot $G_t(\Delta t)$ of the same network. On static networks the occupation probability ρ_k^{static} is the probability the walker is in a given node with degree k, which is proportional to the node degree, i.e., $\rho_k^{\mathrm{static}} \propto k$ [36, 37]. In the limit where the network and the integrating windows are large Eq. (3) simplifies to (see SI)

$$\rho_a \approx \frac{a + \langle a \rangle}{2N\langle a \rangle} \propto a, \tag{4}$$

In order to contrast ρ_k^{static} against ρ_a we exploit the proportionality between the degree of a node v, k_v, and its activity, a_v. In the regime of large Δt, $k_v \propto a_v$ [17]. Combining this result with our derivation in Eq. (4) yields $\rho_{a_v} \propto k_v$, from which we conclude that $\rho_{k_v}^{\mathrm{static}} \propto \rho_{a_v}$ for any node v over any static snapshot $G_t(\Delta t)$, $t = 0, 1, \ldots$. This is an important result that clearly shows how our theory reduces the well-known behavior found in static networks for sufficiently large Δt. In our SI we also show that Eq. (4) holds for a broader range of time-varying aggregations in which integrated edges have weights proportional to their level of activity.

A less intuitive result is found in the regime of very short aggregating windows, $\Delta t \ll 1$. In time-varying dyadic networks when $\Delta t \ll 1$, Eq. (3) simplifies to (see SI)

$$\rho_a \approx \frac{1}{N}\,. \tag{5}$$

Thus, the walker is equally likely to be found at any node regardless of its activity rate. This might appear counterintuitive at first, as one would expect more active nodes to be attractors to the random walker. However, when Δt is small the network is characterized just by dyads and each node has degree either zero or one. Consequently highly active nodes lose and gain walkers at the same rate, giving rise to homogeneous occupation probabilities in Eq. (5). Moreover, Eq. (5) holds even over families of time-varying networks whose aggregated snapshots are strongly correlated (see SI).

The case of bipartite network projections.

Time-varying networks can also be bipartite in nature, typically with one class of nodes representing the actors of a system and the other class representing the groups or objects they interact with [37–39]. Examples are the networks formed by scientific authors and the articles they co-author, listeners and songs, and consumers and products (books, smartphones, etc.). Time-varying edges can only be created between nodes of different classes, but the relationship between actors can be obtained from a simple projection, where all agents connected to the same object form a clique in the network. Similarly, the relationship among objects can also be obtained. Henceforth we denote these networks as *time-varying projected bipartite networks*. Note that unlike time-varying dyadic networks,in time-varying projected bipartite networks nodes form instantaneous cliques of any size.

Interestingly, the walker over such time-varying projected bipartite network turns out to behave much like a walker over a time-varying dyadic network. Let ρ_a^{bp} denote the RW occupation probability on the time-varying projected bipartite network. If $\Delta t \to 0$ it is possible to show that $\rho_a^{\mathrm{bp}} = 1/N$[44] (see SI for complete derivation). This is because the occupation probability is shared among the nodes in the cliques created by the bipartite projections [34], thus resulting in a homogenous distribution of ρ_a. Interestingly, as we will see in the next sections, our experimental results also indicate $\rho_a^{\mathrm{bp}} \propto \rho_a^{\mathrm{dyadic}}$ across a range of values of $\Delta t > 0$, once we adjust for the fact that a time-varying projected bipartite network creates more edges than a time-varying dyadic network with the same activity distribution.

A precise mathematical formulation that derives this relationship between projected bipartite and dyadic networks for arbitrary $\Delta t > 0$ remains an open problem due to the combinatorial difficulties that arise from the growth of clique sizes as Δt gets larger.

Numerical simulations on synthetic networks.

We support our analytical results with extensive Monte Carlo simulations of the RW process with various activity-driven network parameters. We study networks characterized by $N = 10^5$ nodes and a power law activity distribution $dF(a) \propto a^{-\gamma}$ (as observed in many real networks [17]). We restricted the activity to the interval $\Omega = [10^{-3}, 1]$ in order to avoid possible divergencies in the limit $a \ll 1$. As shown in Figure 2-A, the exact solution reproduces the simulations with great accuracy. Note a one-order magnitude increase in Δt (e.g. from $\Delta t = 1$ to $\Delta t = 10$) is enough to elicit a sharp increase in the occupation probability at high-activity nodes. This increase, however, is met with a slight occupation probability reduction at low activity nodes. Also note that as Δt increases $\rho_a \propto a$ approaches a straight line as predicted by Eq. (4). Similarly, as Δt gets smaller, $\rho_a = 1/N$, as predicted by Eq. (5).

We also investigate the relationship between ρ_a and the number of simultaneous connections m. In Figure 2-B we show the results using the same parameters as before but changing the value of m from one to six. The increase in ρ_a at high activity nodes is much smoother than in the previous case $m = 1$. Low (high) activity nodes (whose activity rates are smaller (larger) than the average $\langle a \rangle$) also have lower (higher) occupation probability at $m = 6$ than at $m = 1$. This behavior is puzzling as, by increasing m, we are increasing in equal proportions both the average number of passive and active destinations of all nodes, which (at least in average) would mean no change in occupation probabilities. However, the overall activity on the network increases with m. Thus, walkers at low activity nodes move more quickly, which decreases (increases) the occupation probability at low (high) activity nodes.

Integrating window effects in real datasets.

We also study the impact of integrating windows on the stationary distribution of a RW over two datasets and compare the results with the predictions of our theory. We consider two empirical time-varying (projected) bipartite networks (see Methods for the details). The first is a time-varying co-authorship network of the Physical Review Letters (PRL) journal from 1980 to 2006 [40]. The second consists in the Yahoo! music dataset [41] with approximately 4.6×10^5 songs rated by approximately 2×10^4 Yahoo! users, observed over the course of six months [41] (see Methods for the details). Our experiment consists in running a RW process over these two time-varying networks with different integrating windows Δt and recording the empirical walker occupation probability over multiple runs.

Strikingly, our theoretical predictions match the empirical behavior of the RW process over these real time-varying networks remarkably well. In the case of PRL, we integrate over four distinct values of $\Delta t = \{1, 10, 60, 182\}$ days. The solid points in Figure 3 show the empirical values of ρ_a observed in this dataset. These results are exact (see SI). The standard deviation obtained from simulation runs with distinct starting days are shown as error bars. The solid lines are the numerical solution of Eq. (3), where $Q_{a|a'}(\Delta t)$ is as described in Eq. (2) (that is, we model the network as a time-varying dyadic network), with Δt as a rescaling parameter (see SI). All numerical solutions use the same activity distribution $\mathrm{dF}(a)$, extracted from the time-varying graph of $\Delta t = 1$ day. We note in passing that $\mathrm{dF}(a)$ extracted from larger values of Δt are roughly identical to the one at $\Delta t = 1$, as shown by Perra et al.[17] (see SI for details). Figure 3 shows great agreement between the theoretic results and the simulations in real data. Moreover, for small $\Delta t = 1$ the RW occupation probability is uniform and independent of node activity, as predicted by Eq. (5). Interestingly, for $m > 1$ did not observe good agreement with the theory while for $m = 1$ the data matches well the predicted theoretical behavior, showing an interesting connection between projected bipartite and dyadic time-varying networks.

In the Yahoo! song ratings time-varying network, we use four distinct values of Δt, namely one second, one hour, six hours, and one day. The RW occupation probability ρ_a is shown in Figure 4 as solid points. All numerical solutions use the same activity distribution $\mathrm{dF}(a)$, extracted from the time-varying graph of Δt of one second. Here, as in the PRL experiment, the results are mostly insensitive to the value of Δt chosen to extract $\mathrm{dF}(a)$ (see SI for details). Figure 4 shows that the theoretical results match the real data well, with some deviations for nodes in the intermediate activity range at Δt of one day. As predicted by Eq. (4), as Δt increases the RW occupation probability ρ_a approaches a straight line, and this effect is most prominent at high-activity nodes. Moreover, as in the PRL network, at the smallest value of Δt (one second) the RW occupation probability is uniform and independent of node activity, as predicted by Eq. (5).

Discussion and conclusion

For practical or technical reasons researchers are often forced, or simply tempted, to work with time aggregated representations of time-varying networks. However, such aggregation may impact the behavior of dynamical processes taking place on top of these networks. Motivated by this observation, we have investigated the role played by time aggregation windows on the behavior of random walks, arguably the most widely studied diffusion process.

Our results demonstrate that time aggregation procedures do have a significant impact in the characterization of the dynamical process, even when aggregation windows are "relatively short." We have quantified this effect in a rigorous mathematical framework that (i) allows us to recover the results concerning static networks in the limit of infinite aggregation windows, and (ii) accurately describes the behavior observed in numerical simulations upon synthetic time-varying networks. Moreover, testing our predictions against real datasets we have shown that our model captures well the observed phenomenology, not only qualitatively but also quantitatively.

Overall, our work suggests that caution should be used when drawing general conclusions about dynamical processes on time-varying graphs extrapolated from their study on time-aggregated networks. At the same time, however, our theoretical results may help to investigate possible distortions introduced by the aggregating windows of data collection methods.

Methods

Activity-driven networks.

Activity-driven network models are based on the activity patterns of nodes, that are used to explicitly model the evolution of the network structure over time [17]. Each node i is characterized by an activity rate a_i, sampled from distribution $\mathrm{dF}(a)$. At each step $t = 0, 1, \ldots$ the network $G_t(\Delta t)$ is generated as follows:

a) $G_t(\Delta t)$ starts with N disconnected nodes;

b) The the number of times a node with activity a is *active* during interval Δt, $K_{\Delta t,a}$, is Poisson distributed

$$\mathrm{P}[K_{\Delta t,a} = k] = \frac{(a\Delta t)^k}{k!} \exp(-a\Delta t).$$

Node generates $mK_{\Delta t,a}$ undirected edges connected to $mK_{\Delta t,a}$ randomly selected nodes (without replacement or self-loops). Parameter m represent the average number of instantaneous connections established by each active node in the system. Inactive nodes in this observed period of Δt may receive connections from other active vertices;

c) At time $(t + 1)\Delta t$ the process starts over from step a) to generate network $G_{t+1}(\Delta t)$.

It can be shown that the full dynamics of the network are encoded in the activity rate distribution, $\mathrm{dF}(a)$ and that the time-aggregated measurement of network connectivity yields a degree distribution that follows the same functional form as the distribution $\mathrm{dF}(a)$ in the limit of small $k/\Delta t$ and k/N [17]. This is an important feature of the model, that is able to reproduce basic statistical properties found in many real networks giving a simple prescription to characterize explicitly dynamical connectivity patterns.

Datasets & Simulation.

In this study we considered two different empirical projections of bipartite time-varying networks. The collaborations in the journal Physical Review Letters (PRL) published by the American Physical Society [40], and the Yahoo! music dataset made available by Yahoo! [41].

PRL dataset. The bipartite network representation of this dataset has two type of nodes: authors and papers. An author is connected to all the papers she/he wrote in a integrating window Δt. We study the bipartite projection of the authors. In this representation each author of an article in PRL as a node. Undirected edges connect authors that collaborate in the same article. We focus just on small collaborations filtering out all the articles with more

than 10 authors. We consider the period between 1958 and 2006. The datasets contains 80,554 authors and 66,892 articles. The smallest timescale available is one day.

Yahoo! music dataset. In this dataset the bipartite network has two type of nodes: users and songs. We study the bipartite projection over the songs. Each node is a song and two songs are connected if at least one user rated both in a time window Δt. The dataset contains 4.6×10^5 songs rated by 199,719 users of Yahoo! users collected in the course of six months [41]. User activity is recorded at a time resolution of seconds.
Simulation setup. We obtain the empirical walker occupation probability, ρ_a, as follows. Construct the transition probability matrix P_t associated to the RW on the t-th aggregated network $G_t(\Delta t)$, $t = 0, \ldots, \lfloor T/\Delta t \rfloor$, where T is the time of the last event in the dataset. The empirical RW occupation probability is obtained by multiplying the matrices $P_0\, P_1 \cdots P_n$ and then left-multiplying the result by the vector $(1/N, \ldots, 1/N)$, which gives equal probability that for the walker to start at any node. We note in passing that similar results are obtained when the walker starts at a handful of high activity nodes.

[1] Holme, P. & Saramäki, J. Temporal networks. *Phys. Rep.* **519**, 97 (2012).
[2] Morris, M. Telling tails explain the discrepancy in sexual partner reports. *Nature* **365**, 437 (1993).
[3] Morris, M. *Sexually Transmitted Diseases, K.K. Holmes, et al. Eds.* (McGraw-Hill, 2007).
[4] Clauset, A. & Eagle, N. Persistence and periodicity in a dynamic proximity network. In *DIMACS Workshop on Computational Methods for Dynamic Interaction Networks*, 1–5 (2007).
[5] Vespignani, A. Modeling dynamical processes in complex socio-technical systems. *Nature Physics* **8**, 32–30 (2012).
[6] Rocha, L. E. C., Liljeros, F. & Holme, P. Simulated epidemics in an empirical spatiotemporal network of 50,185 sexual contacts. *PLoS Comput Biol* **7**, e1001109 (2011).
[7] Isella, L. *et al.* What's in a crowd? analysis of face-to-face behavioral networks. *J. Theor. Biol* **271**, 166 (2011).
[8] Stehlé, J. *et al.* Simulation of an seir infectious disease model on the dynamic contact network of conference attendees. *BMC Medicine* **9** (2011). URL `http://www.biomedcentral.com/1741-7015/9/87`.
[9] Karsai, M. *et al.* Small but slow world: How network topology and burstiness slow down spreading. *Phys. Rev. E* **83**, 025102 (2011). URL `http://link.aps.org/doi/10.1103/PhysRevE.83.025102`.
[10] Miritello, G., Moro, E. & Lara, R. Dynamical strength of social ties in information spreading. *Phys. Rev. E* **83**, 045102 (2011). URL `http://link.aps.org/doi/10.1103/PhysRevE.83.045102`.
[11] Kivela, M. *et al.* Multiscale analysis of spreading in a large communication network (2011). ArXiv:1112.4312v1.
[12] Fujiwara, N., Kurths, J. & Díaz-Guilera, A. Synchronization in networks of mobile oscillators. *Physical Review E* **83**, 025101 (2011).
[13] Parshani, R., Dickison, M., Cohen, R., Stanley, H. E. & Havlin, S. Dynamic networks and directed percolation. *EPL (Europhysics Letters)* **90**, 38004 (2010). URL `http://stacks.iop.org/0295-5075/90/i=3/a=38004`.
[14] Bajardi, P., Barrat, A., Natale, F., Savini, L. & Colizza, V. Dynamical patterns of cattle trade movements. *PLoS ONE* **6**, e19869 (2011).
[15] Baronchelli, A. & Díaz-Guilera, A. Consensus in networks of mobile communicating agents. *Phys. Rev. E* **85**, 016113 (2012).
[16] Starnini, M., Baronchelli, A., Barrat, A. & Pastor-Satorras, R. Random walks on temporal networks. *Phys. Rev. E* **85**, 056115 (2012).
[17] Perra, N., Gonçalves, B., Pastor-Satorras, R. & Vespignani, A. Time scales and dynamical processes in activity driven networks. *Scientific Reports* **2**, 469 (2012).
[18] Perra, N. *et al.* Random walks and search in time varying networks. *Phys. Rev. Lett.* **109**, 238701 (2012).
[19] Hoffmann, T., Porter, M. & Lambiotte, R. Generalized master equations for non-poisson dynamics on networks. *Physical Review E* **86**, 046102 (2012).
[20] Butts, C. Relational event framework for social action. *Sociological Methodology* **38**, 155–200 (2008).
[21] Toroczkai, Z. & Guclu, H. Proximity networks and epidemics. *Physica A* **378**, 68–75 (2007).
[22] Maity, S., Manoj, T. & Mukherjee, A. Opinion formation in time-varying social networks: The case of the naming game. *Physical Review E* **86**, 036110 (2012).
[23] Carley, K. Dynamics network analysis. 133–145 (2003).
[24] Rosvall, M. & Bergstrom, C. T. Mapping change in large networks. *PLoS ONE* **5:e8694** (2010).
[25] Holme, P. *et al.* On network bipartivity. *e-print cond-mat/0302296* (2003).
[26] Cattuto, C. *et al.* Dynamics of person-to-person interactions from distributed rfid sensor networks. *PloS One* **5**, e11596 (2010).
[27] Redner, S. How popular is your paper? An empirical study of the citation distribution. *Eur. Phys. J. B* **4**, 131–134 (1998).
[28] Radicchi, F., Fortunato, S., Markines, B. & Vespignani, A. Diffusion of scientific credits and the ranking of scientists. *Phys. Rev. E* **80**, 056103 (2009).
[29] Pan, R. K., Kaski, K. & Fortunato, S. World citation and collaboration networks: uncovering the role of geography in science. arXiv:1209.0781v1 (2012).

[30] Java, A., Song, X., Finin, T. & Tseng, B. Why we twitter understanding microblogging usage and communities. In *In proceedings of the 9th WebKDD and 1st SNA-KDD workshop on web mining and social network analysis* (2007).
[31] Kumar, R., Novak, J. & Raghavan P. Tomkins, A. On the bursty evolution of blogspace. In *In proceedings of the 12th international conference of world wide web* (2003).
[32] Onnela, J.-P. *et al.* Structure and tie strengths in mobile communication networks. *Proc. Natl. Acad. Sci. U.S.A.* **104**, 7332 (2007).
[33] Wu, Y., Zhou, C., J, X., Kurths, J. & Schellnhuber, H. Evidence for a bimodal distribution in human communication. *Proc. Natl. Acad. Sci. U.S.A.* **107**, 18808–18808 (2010).
[34] Figueiredo, D., Nain, P., Ribeiro, B., de Souza, E. & Towsley, D. Characterizing continuous time random walks on time varying graphs. *SIGMETRICS* 203–207 (2012).
[35] Feller, W. *An introduction to probability theory and its applications. Vol. II.* Second Ed. (John Wiley & Sons Inc., New York, 1971).
[36] Noh, J. & Rieger, H. Random walks on complex networks. *Phys. Rev. Lett.* **92**, 118701 (2004).
[37] Barrat, A., Barthélemy, M. & Vespignani, A. *Dynamical Processes on Complex Networks* (Cambridge Univesity Press, 2008).
[38] Newman, M. *Networks. An Introduction* (Oxford Univesity Press, 2010).
[39] Caldarelli, G. *Scale-Free Networks* (Oxford University Press, 2007).
[40] APS. Data sets for research (2010).
[41] Yahoo! webscope dataset ydata-ymusic-kddcup-2011-track1. URL `http://labs.yahoo.com/Academic_Relations`.
[42] Growing networks may also be contemplated by this model by starting the time-varying network with $N \gg 1$ disconnected nodes. A node arrival is then equivalent to an edge arrival to a previously never-connected node.
[43] $\mathrm{dF}(a)$ is a Lesbegue measurable function so that our framework seamlessly treats the case where activity rates are discrete or are not amenable to density functions (e.g. when the network is small).
[44] This result holds over any stationary and ergodic time-varying bipartite network.

Supporting Information

The SI is available at `www.nicolaperra.com/si.html`

Acknowledgments

We would like to thank Yahoo! for kindly providing data used in this study. The work has been partly sponsored by the Army Research Laboratory and was accomplished under Cooperative Agreement Number W911NF-09-2-0053. B.R. was also supported by the NSF grant CNS-1065133. The views and conclusions contained in this document are those of the authors and should not be interpreted as representing official policies, either expressed or implied of the NSF, Army Research Laboratory, or the U.S. Government. The U.S. Government is authorized to reproduce and distribute reprints for Government purposes notwithstanding any copyright notation hereon.

Author Contributions

All the authors designed research. B.R. developed the mathematical formalism and derived the analytical results. B.R. & N.P. performed numerical simulations. All the authors analyzed the results, wrote, reviewed and approved the manuscript.

Competing financial interests

The authors declare no competing financial interests.

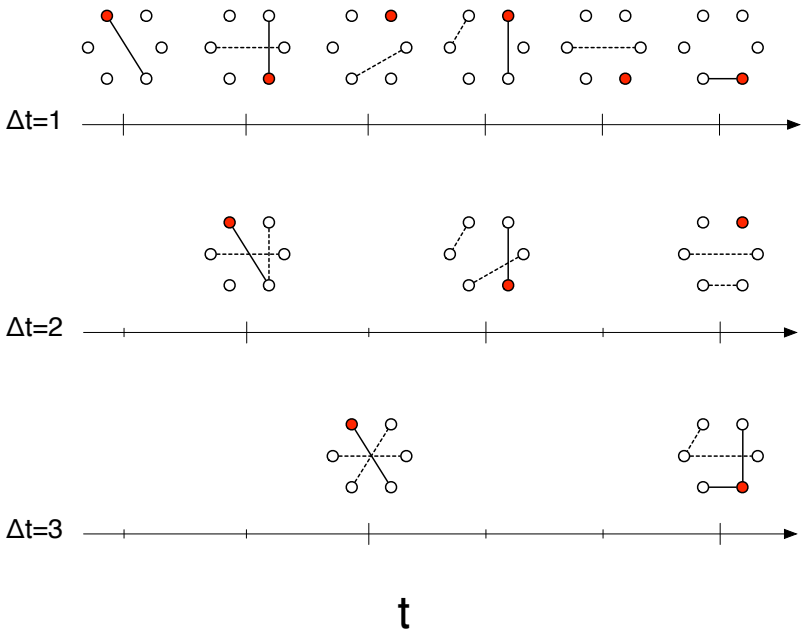

FIG. 1: Example of time integration on time-varying networks. The random walker is located at the red node and Δt defines integration window.

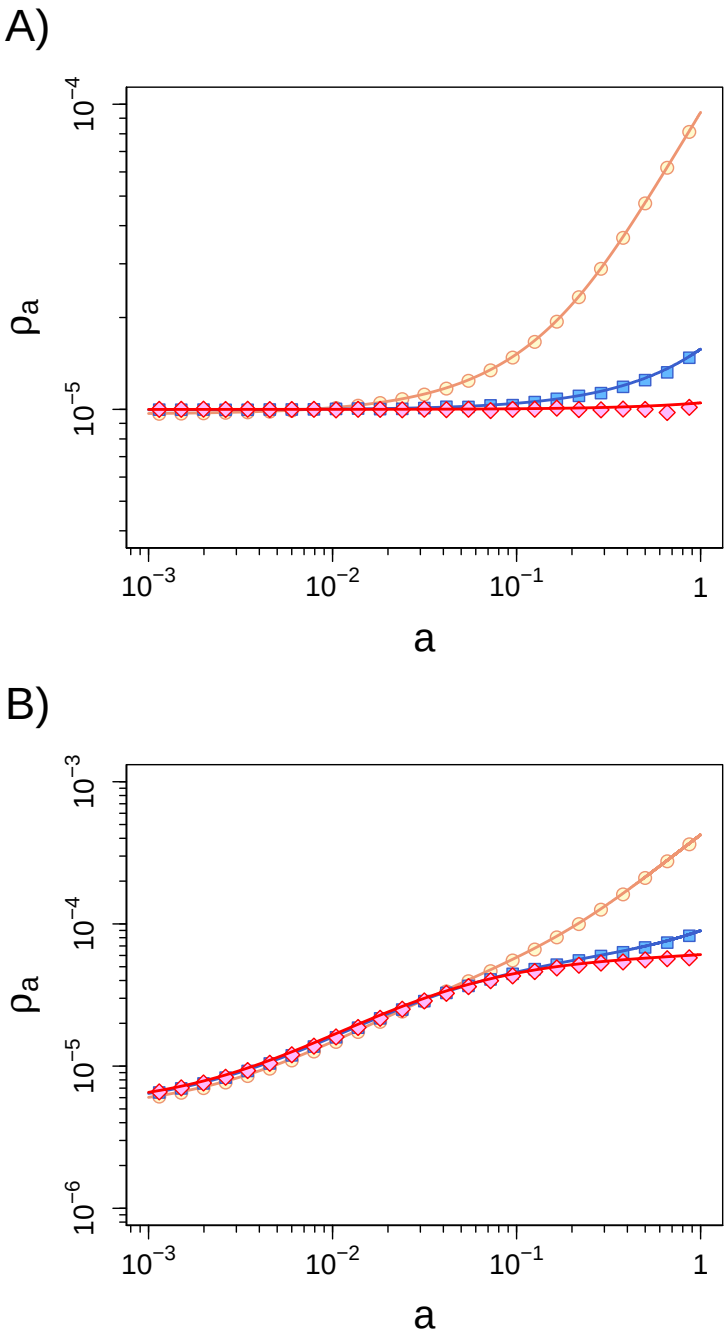

FIG. 2: Occupation probability ρ_a of a RW over an activity-driven network with activity distribution $dF(a) \propto a^{-2}$, $a \in (10^{-3}, 1)$, $N = 10^5$, for different values of m. In panel A) we plot the results for $m = 1$. In panel B) instead, $m = 6$. Solid lines represent the analytical prediction Eq. (3) integrated over $\Delta t = 1, 10, 100$ (diamonds, squares and circles) time windows. Note that in both panels as Δt gets larger $\rho_a \approx a$. Averages performed over 10^3 independent simulations.

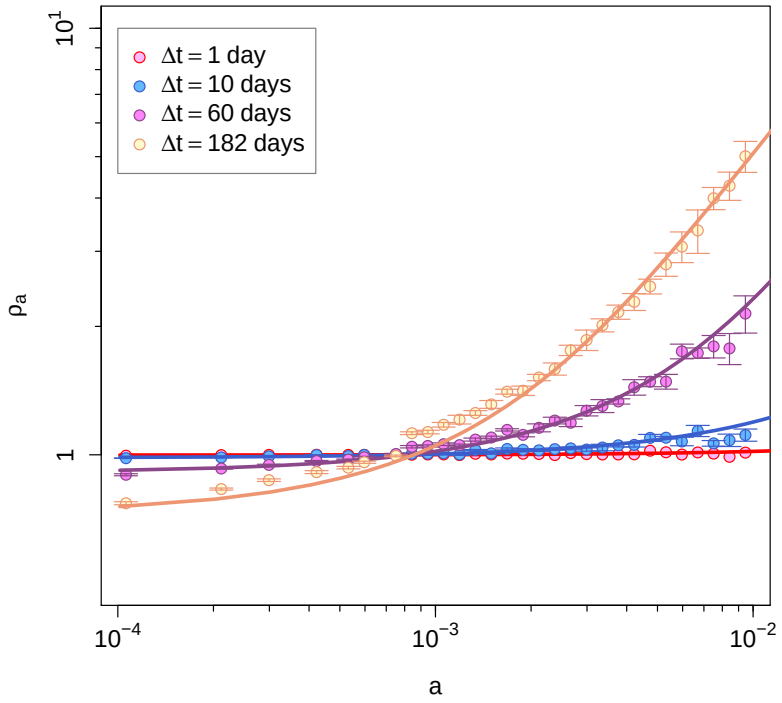

FIG. 3: Occupation probability ρ_a of a RW at the end of the simulation as a function of node activity. The points are the values of ρ_a on the Physics Review Letters time-varying co-authorship network from 1980 to 2006 for different integrating windows $\Delta t \in \{1, 10, 60, 182\}$ days. The solid lines are the numerical solution of Eq. (3). The error bars are evaluated starting the process at different starting points.

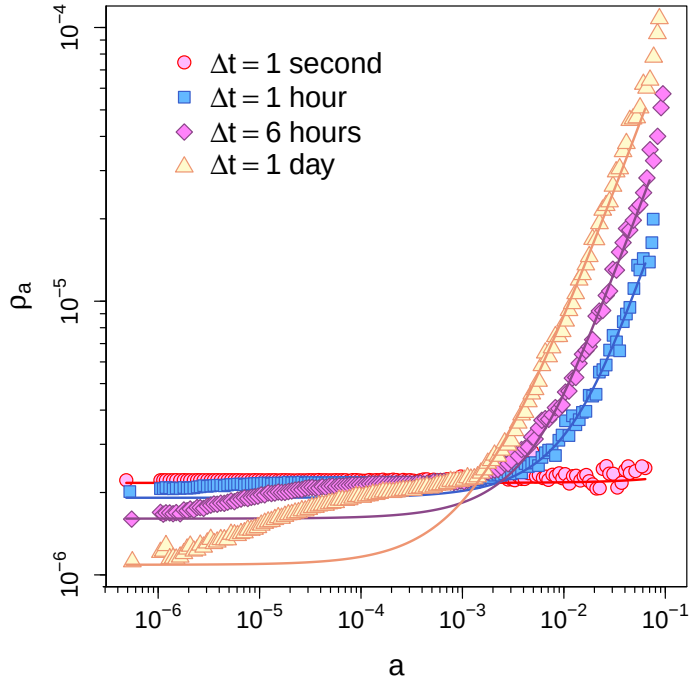

FIG. 4: Occupation probability ρ_a of a RW at the end of the simulation as a function of node activity. The points are the values of ρ_a on the time-varying graph of Yahoo! song ratings for different integrating windows Δt of one second, one hour, six hours, and one day. The solid lines are the numerical solution of Eq. (3). The standard deviations are too small to be shown in the plots.